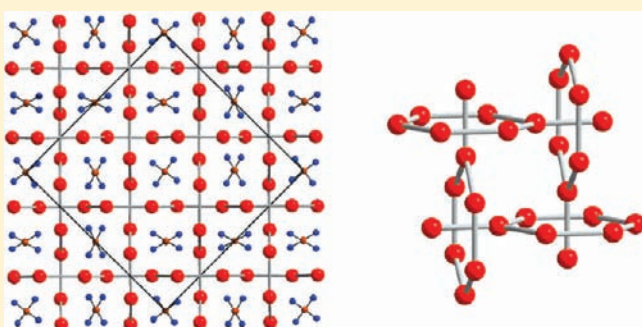


Refined Crystal Structure and Idealized Structure of Mixed-Valent  $\text{Eu}_4\text{F}_5(\text{CN}_2)_2$ : Transition PossibleLeonid Unverferth,<sup>†</sup> Markus Ströbele,<sup>†</sup> Jochen Glaser,<sup>†</sup> Thorsten Langer,<sup>‡</sup> Rolf-Dieter Hoffmann,<sup>‡</sup> Rainer Pöttgen,<sup>\*,‡</sup> and H.-Jürgen Meyer<sup>\*,†</sup><sup>†</sup>Abteilung für Festkörperchemie und Theoretische Anorganische Chemie, Institut für Anorganische Chemie, Universität Tübingen, Ob dem Himmelreich 7, 72074 Tübingen, Germany<sup>‡</sup>Institut für Anorganische und Analytische Chemie, Westfälische Wilhelms-Universität Münster, Corrensstrasse 30, 48149 Münster, Germany

## Supporting Information

**ABSTRACT:** The new europium fluoride carbodiimide  $\text{Eu}_4\text{F}_5(\text{CN}_2)_2$  was synthesized by solid state reaction from mixtures of  $\text{EuF}_3$  and  $\text{Li}_2(\text{CN}_2)$  at 700 °C. The crystal structure as refined by single crystal X-ray diffraction ( $P\bar{4}2_1c$ , no. 114,  $a = 16.053(1)$  Å,  $c = 6.5150(6)$  Å,  $Z = 8$ ) reveals three crystallographically distinct  $[\text{N}=\text{C}=\text{N}]^{2-}$  ions in the structure of mixed-valent  $\text{Eu}_4\text{F}_5(\text{CN}_2)_2$ . The presence of one  $\text{Eu}^{3+}$  and three  $\text{Eu}^{2+}$  per formula unit  $\text{Eu}_4\text{F}_5(\text{CN}_2)_2$  is confirmed by magnetic measurements and  $^{151}\text{Eu}$ -Mössbauer spectroscopy. The arrangement of Eu ions and gravity centers of  $[\text{NCN}]^{2-}$  ions in the structure of  $\text{Eu}_4\text{F}_5(\text{CN}_2)_2$  follow the motif formed by atoms in the  $\text{CuAl}_2$ -type structure. A possible high-symmetry structure of  $\text{Eu}_4\text{F}_5(\text{CN}_2)_2$  is discussed on the basis of a group-subgroup scheme.



## INTRODUCTION

An increasing number of metal carbodiimide compounds have been reported during the past years. The discovery of thermally moderately stable rare-earth (RE) carbodiimide compounds was significantly promoted by the approach of straightforward solid-state metathesis (SSM) reactions.<sup>1</sup> However, some examples of SSM reactions between transition metal halides and alkali carbodiimide have also demonstrated the reducing potential of the carbodiimide ion, thereby producing nitride or carbide containing compounds. For example, reactions of tungsten hexachloride with lithium carbodiimide yielded the mixed-valent tungsten(V,VI) nitride chloride  $\text{W}_2\text{NCl}_8$ <sup>2</sup> and the carbon-centered cluster compound  $\text{Li}[\text{W}_6\text{CCl}_{18}]$ ,<sup>3</sup> respectively. In contrast, the more electronegative transition elements  $M = \text{Mn}, \text{Fe}, \text{Co}, \text{Ni},$  and  $\text{Cu}$  form divalent carbodiimide compounds  $\text{M}(\text{CN}_2)$ , as synthesized via aqueous solution routes or by metathesis reactions.<sup>4–7</sup>

The number of RE carbodiimide compounds grew rapidly within the past few years being represented by the series of quasi binary RE carbodiimide compounds  $\text{RE}_2(\text{CN}_2)_3$  ( $\text{RE} = \text{Y}, \text{Ce}–\text{Lu}$ )<sup>8</sup> and by other compositions containing additional constituents, such as nitride in  $\text{RE}_3(\text{CN}_2)_3\text{N}$ , or lithium in  $\text{LiRE}(\text{CN}_2)_2$ .<sup>9</sup> Moreover, halide containing compounds such as  $\text{REX}(\text{CN}_2)$ <sup>10</sup> or  $\text{RE}_2\text{X}(\text{CN}_2)\text{N}$ <sup>11</sup> ( $\text{X} = \text{F}, \text{Cl}, \text{Br},$  or  $\text{I}$ ) were results of systematically modified starting compositions of reaction partners ( $\text{REX}_3$ ,  $\text{Li}_2(\text{CN}_2)$ , and  $\text{Li}_3\text{N}$ ) employed in SSM reactions. Luminescence properties were reported some time ago for

doped  $\text{RE}_2\text{O}_2(\text{CN}_2)$  compounds,<sup>12</sup> followed by more recent examples of RE oxide carbodiimides.<sup>13</sup> Cerium-doped  $\text{RE}_2(\text{CN}_2)_3$  compounds ( $\text{RE} = \text{Y}, \text{La}$ ) exhibit broad-band emissions, being slightly red-shifted compared with the most widely used LED emitter  $\text{YAG}:\text{Ce}$ .<sup>14</sup>

Most europium carbodiimide halides reported to date, such as  $\text{LiEu}(\text{CN}_2)\text{I}$ ,  $\text{LiEu}_2(\text{CN}_2)\text{I}_3$ ,  $\text{LiEu}_4(\text{CN}_2)_3\text{I}_3$ ,<sup>15</sup>  $\text{LiEu}_2(\text{CN}_2)\text{Br}_3$ ,<sup>16</sup> or  $\text{Eu}_2\text{Cl}_2(\text{CN}_2)$ <sup>17</sup> contain divalent europium. We note here, that the formula notations of these compounds differ sometimes with respect to the sequence of anions being given in a formula.<sup>18</sup>

The electronic configuration of europium compounds can be regarded either as divalent or trivalent. Generally this issue may be controlled by synthesis, like for the well-known examples  $\text{EuF}_2$  and  $\text{EuF}_3$ , or for the europium carbodiimide compounds  $\text{Eu}(\text{CN}_2)$ <sup>19</sup> and  $\text{Eu}_2(\text{CN}_2)_3$ ,<sup>20</sup> respectively. After carbodiimide ions have been frequently considered as pseudo chalcogenide ions, we want to refer to europium sulphides being divalent ( $\text{EuS}$ ), trivalent ( $\text{Eu}_2\text{S}_3$ ), and also mixed-valent ( $\text{Eu}_3\text{S}_4$ ).  $\text{Eu}_3\text{S}_4$  can be considered as a prototype of a mixed-valent compound showing a charge ordering transition on cooling the cubic ( $I\bar{4}3d$ )  $\text{Th}_3\text{P}_4$  type structure below 160 K to yield a tetragonally ( $I\bar{4}2d$ ) distorted structure.<sup>21</sup>

Received: December 22, 2010

Published: June 09, 2011

**Table 1.** Crystal Data from the Single Crystal Structure Refinement of  $\text{Eu}_4\text{F}_5(\text{CN}_2)_2$ 

	chemical formula
	$\text{Eu}_4\text{F}_5(\text{CN}_2)_2$
crystal system	tetragonal
<i>a</i>	16.053(1) Å
<i>c</i>	6.5150(6) Å
<i>V</i>	1678.8(3) Å <sup>3</sup>
<i>Z</i>	8
formula weight	782.90 g/mol
space group	$P4_21c$
Flack parameter	0.00(2)
<i>T</i>	293(2) K
$\lambda$	0.71073 Å
$d_{\text{calc}}$	6.20 g/cm <sup>3</sup>
$\mu$	29.5 mm <sup>-1</sup>
$R_1, wR_2$ (all data)	0.0275, 0.0459

Mixed-valent europium compounds are well-known from several examples, such as  $\text{Eu}_2\text{O}_2\text{Br}$ ,<sup>22</sup>  $\text{Na}_5\text{Eu}_7\text{Cl}_{22}$ ,<sup>23</sup> and  $\text{Eu}_5\text{F}[\text{SiO}_4]_3$ <sup>24</sup> in whose structures separate lattice sites can be addressed to  $\text{Eu}^{2+}$  and  $\text{Eu}^{3+}$  ions, respectively. Compounds like these account for inhomogeneous mixed-valence compounds, where charge fluctuations are considered as being frozen. The colors of crystalline materials were reported as red ( $\text{Eu}_2\text{O}_2\text{Br}$ ,  $\text{Eu}_5\text{F}[\text{SiO}_4]_3$ ) or violet ( $\text{Na}_5\text{Eu}_7\text{Cl}_{22}$ ).

Herein we report on the synthesis and characterization of the first mixed-valent carbodiimide  $\text{Eu}_4\text{F}_5(\text{CN}_2)_2$ .

## EXPERIMENTAL SECTION

**Synthesis.** All manipulations of compounds were carried out in an argon filled glovebox. Preparations of  $\text{Eu}_4\text{F}_5(\text{CN}_2)_2$  were performed departing from mixtures of  $\text{EuF}_3$ ,  $\text{EuF}_2$ , and  $\text{Li}_2(\text{CN}_2)$ . Reaction mixtures were loaded into arc-welded copper tubes which were then fused into evacuated silica tubes. Europium difluoride was obtained via hydrogen reduction of  $\text{EuF}_3$  (NOXAL, 7%  $\text{H}_2$  in Ar) at 700 °C, and is known to have a phase-width corresponding to  $\text{EuF}_{2+x}$ <sup>25</sup> denoted as  $\text{EuF}_2$  in our reactions.

**Magnetism.** Three samples prepared by different reactions (eqs I–III) were used for magnetic measurements using a SQUID magnetometer (Quantum Design, MPMS) between room temperature and 5 K. Samples were weighted into gelatin capsules and after cooling down to 5 K a magnetic field of 100 Oe was applied. The magnetic susceptibility was measured at several temperatures while heating the samples up to room temperature (zero field cooled ZFC). Measurements in the applied magnetic field while cooling the samples down to 5 K resulted in the field cooled magnetic susceptibility (FC).

**<sup>151</sup>Eu–Mössbauer Spectroscopy.** The 21.53 keV transition of <sup>151</sup>Eu with an activity of 130 MBq (2% of the total activity of a <sup>151</sup>Sm:  $\text{EuF}_3$  source) was used for the Mössbauer spectroscopic experiments which were conducted in the usual transmission geometry. The measurements were performed on samples I and II with a commercial helium-bath cryostat. The temperature of the absorber was varied between 4.2 and 330 K, while the source was kept at room temperature. The temperature was controlled by a resistance thermometer ( $\pm 0.5$  K accuracy). The samples were enclosed in small PVC containers at a thickness corresponding to about 10 mg Eu/cm<sup>2</sup>.

**X-ray Diffraction.** Red-transparent single-crystals of  $\text{Eu}_4\text{F}_5(\text{CN}_2)_2$  were selected in air and fixed on the tip of a glass fiber for a single-crystal

**Table 2.** Atom Positions and Isotropic Equivalent Displacement Parameters (Å<sup>2</sup>) in the Crystal Structure of  $\text{Eu}_4\text{F}_5(\text{CN}_2)_2$ 

	Wyckoff site	<i>x</i>	<i>y</i>	<i>z</i>	$U_{\text{eq}}$
Eu(1)	8e	0.4136(1)	0.1653(1)	0.0090(1)	0.0092(1)
Eu(2)	8e	0.6683(1)	0.0804(1)	0.0173(1)	0.0104(1)
Eu(3)	8e	0.4200(1)	0.3328(1)	0.5114(1)	0.0108(1)
Eu(4)	8e	0.3266(1)	0.4220(1)	−0.0043(1)	0.0117(1)
F(1)	8e	0.2448(2)	0.5040(2)	−0.2521(4)	0.0139(9)
F(2)	8e	0.3166(3)	0.4302(3)	0.3702(5)	0.0142(7)
F(3)	8e	0.3166(3)	0.0674(3)	0.1344(5)	0.0140(7)
F(4)	8e	0.5545(2)	0.1719(2)	−0.0970(6)	0.016(1)
F(5)	8e	0.4243(3)	0.3078(3)	−0.0936(5)	0.0171(9)
C(1)	4d	1/2	0	0.291(2)	0.020(3)
C(2)	8e	0.2512(4)	0.2450(4)	0.271(2)	0.008(2)
C(3)	4c	1/2	1/2	−0.264(2)	0.023(4)
N(1)	8e	0.2361(4)	0.3210(5)	−0.240(1)	0.024(2)
N(2)	8e	0.4254(5)	0.4885(4)	−0.2626(8)	0.023(2)
N(3)	8e	0.4764(4)	0.0726(4)	0.289(1)	0.021(1)
N(4)	8e	0.3247(4)	0.2249(4)	0.2950(9)	0.021(1)

diffraction measurement (Stoe IPDS diffractometer, graphite monochromatized Mo- $K_{\alpha}$  radiation) at room temperature (Table 1). Intensities were corrected for Lorentz factors, polarization and absorption effects.  $\text{Eu}_4\text{F}_5(\text{CN}_2)_2$  was found to crystallize tetragonally with the space group  $P4_21c$ . Structure refinement and anisotropic refinements were performed with the program SHELX.<sup>26</sup> Atom positions are given in Table 2, and selected interatomic distances are provided in Table 3.

The X-ray powder diffraction data of all samples were collected on a Stoe StadiP diffractometer using Ge-monochromatized Cu- $K_{\alpha 1}$  radiation.  $\text{Eu}_4\text{F}_5(\text{CN}_2)_2$  was indexed tetragonally using the lattice parameters of the single crystal measurements. By-products were identified comparing the powder patterns with the entries [4-857] (LiF) and [26-625] ( $\text{EuF}_{2.25}$ ) of the Powder Diffraction File (PDF).

## RESULTS AND DISCUSSION

**Synthesis.** Recent explorations of SSM reactions between RE trifluorides and  $\text{Li}_2(\text{CN}_2)$  have brought up the first examples of RE fluoride carbodiimides, namely, of  $\text{LaF}(\text{CN}_2)$  and of  $\text{LiRE}_2\text{F}_3(\text{CN}_2)_2$  with RE = Ce, Pr, Nd, Sm, Eu, Gd. The synthesis of  $\text{LiEu}_2\text{F}_3(\text{CN}_2)_2$  containing trivalent europium was accomplished between 500 and 600 °C.<sup>20</sup> In the course of these reactions, the new compound  $\text{Eu}_4\text{F}_5(\text{CN}_2)_2$  was first obtained from an approximately 1:1 molar mixture of  $\text{EuF}_3$  and  $\text{Li}_2(\text{CN}_2)$  being heated for 4 days in a fused copper tube at 700 °C.

We already noted in our introductory part that carbodiimide ions can inflate their reducing nature, thereby decomposing into miscellaneous components. Therefore, it can be reasonably assumed that carbodiimide ions can initiate the reduction of trivalent europium into divalent europium at elevated temperatures. Thus, the present synthesis of  $\text{Eu}_4\text{F}_5(\text{CN}_2)_2$  involves a SSM reaction with a simultaneous autoreduction process.

$\text{Eu}_4\text{F}_5(\text{CN}_2)_2$  samples were prepared according to the compositions given in reactions I–III at 650 °C over 3 days, with nominal or expected reaction products as follows:

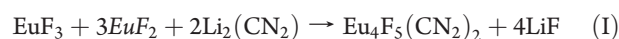
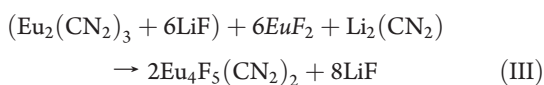
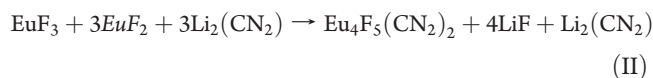


**Table 3.** Selected Interatomic Distances (Å) in the Structure of  $\text{Eu}_4\text{F}_5(\text{CN}_2)_2$ 

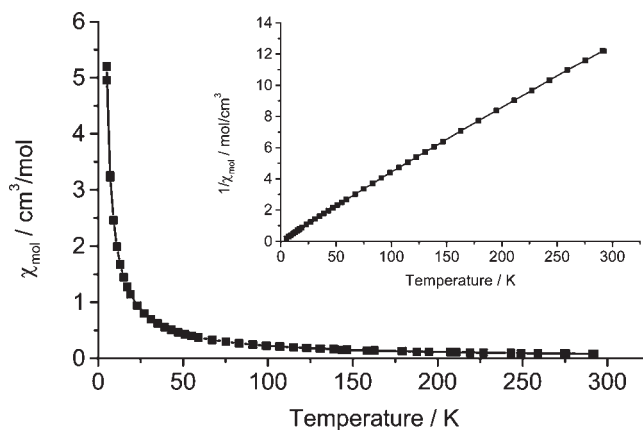
Eu(1)–F(1)	2.426(3)
Eu(1)–F(3)	2.359(4), 2.477(3)
Eu(1)–F(4)	2.366(4)
Eu(1)–F(5)	2.389(4)
Eu(1)–N(3)	2.560(6), 2.699(6)
Eu(1)–N(4)	2.534(6), 2.629(6)
Eu(2)–F(1)	2.516(3)
Eu(2)–F(2)	2.496(5)
Eu(2)–F(3)	2.504(5)
Eu(2)–F(4)	2.460(4), 2.548(4)
Eu(2)–N(1)	2.638(7), 2.894(7)
Eu(2)–N(3)	2.715(6)
Eu(3)–F(1)	2.518(3)
Eu(3)–F(2)	2.458(4), 2.540(5)
Eu(3)–F(3)	2.536(4)
Eu(3)–F(5)	2.605(4)
Eu(3)–N(2)	2.645(6), 2.901(7)
Eu(3)–N(4)	2.707(6)
Eu(4)–F(1)	2.462(3)
Eu(4)–F(2)	2.448(3)
Eu(4)–F(4)	2.597(4)
Eu(4)–F(5)	2.481(4), 2.567(4)
Eu(4)–N(1)	2.662(6)
Eu(4)–N(2)	2.547(6)



An incomplete reaction with the formation of  $\text{Eu}_2(\text{CN}_2)_3$  and  $\text{EuF}_2$  was obtained when reaction I was performed at 550 °C. A residue of europium difluoride (estimated up to 20% by comparing the strongest X-ray reflections) was present even when reaction I was performed at 650 °C. Therefore, an excess of  $\text{Li}_2(\text{CN}_2)$  was attempted in reaction II which was fully consumed during the reaction (eventually for the reduction of  $\text{EuF}_{2+x}$ ). Finally,  $\text{Eu}_2(\text{CN}_2)_3$  was prepared as a starting material (following:  $2\text{EuF}_3 + 3\text{Li}_2(\text{CN}_2) \rightarrow \text{Eu}_2(\text{CN}_2)_3 + 6\text{LiF}$ )<sup>14</sup> and employed in reaction III (without washing off the coproduced LiF).

The products of reactions I–III showed an estimated X-ray phase purity of >90 mass-% of  $\text{Eu}_4\text{F}_5(\text{CN}_2)_2$  with respect to the europium compounds in the systems. The europium difluoride being present in the product of reaction I can be assumed as a mixed-valence europium fluoride that may be indexed rhombohedrally, related to  $\text{EuF}_{2.25}$ – $\text{EuF}_{2.40}$  phases reported in the literature.<sup>25</sup>

Single-crystals of  $\text{Eu}_4\text{F}_5(\text{CN}_2)_2$  were grown from a 1:3:3 mixture of  $\text{EuF}_3$ ,  $\text{EuF}_2$ , and  $\text{Li}_2(\text{CN}_2)$  as red, sometimes dark-red to opaque blocks. Crystals of  $\text{Eu}_4\text{F}_5(\text{CN}_2)_2$  were gathered

**Figure 1.** Temperature dependence of the magnetic susceptibility ( $\chi(T)$ -plot; ZFC and FC) of  $\text{Eu}_4\text{F}_5(\text{CN}_2)_2$  (sample from reaction I) measured in a field of 100 Oe. A  $1/\chi$  vs  $T$  plot is shown in the inset.

by washing reaction products first in water and then with ethanol. Results of the single-crystal measurement and the structure refinement are given in Table 1, atom positions in Table 2, and selected interatomic distances in Table 3.

**Magnetism.** The masses of the byproduct were taken into account when calculating the molar magnetic susceptibilities of  $\text{Eu}_4\text{F}_5(\text{CN}_2)_2$ . The  $1/\chi$  versus  $T$  plots of all samples are almost linear and did not indicate any coupling effects such as ferro- or antiferromagnetism (Figure 1) down to 5 K. Fitting the  $\chi(T)$ -measurements of the samples was performed using an extended Curie–Weiss law, separating the temperature-independent contributions of  $\text{Eu}^{3+}$ . Experimental magnetic moments between 12.5  $\mu_B$  and 13.3  $\mu_B$  per formula unit  $\text{Eu}_4\text{F}_5(\text{CN}_2)_2$  were obtained for the samples (I–III). These values are in good agreement with the expected value of 13.75  $\mu_B$  for 3  $\text{Eu}^{2+}$  per formula unit  $\text{Eu}_4\text{F}_5(\text{CN}_2)_2$ , taking into account that  $\text{Eu}^{3+}$  is known not to have a temperature-dependent contribution to the magnetic susceptibility.<sup>27</sup>

**<sup>151</sup>Eu–Mössbauer Spectroscopy.** The <sup>151</sup>Eu Mössbauer spectra of two different  $\text{Eu}_4\text{F}_5(\text{CN}_2)_2$  samples are provided in Figure 2 together with transmission integral fits. The corresponding fitting parameters are listed in Table 4. All spectra could be well reproduced with two well separated signals which are both subjected to weak quadrupole splitting. Both samples contained a small amount of a secondary  $\text{Eu}^{2+}$  phase. This is readily visible in the spectra. In all cases, the  $\text{Eu}^{2+}$  line width is significantly higher than the  $\text{Eu}^{3+}$  one (Table 4). Most likely the  $\text{Eu}^{2+}$  signals of  $\text{Eu}_4\text{F}_5(\text{CN}_2)_2$  and the  $\text{Eu}^{2+}$  secondary phase have only slightly different isomer shifts ( $\text{EuF}_2$  has a similar  $\delta$  value<sup>28</sup>), and this is manifested in an overlap, resulting in the increased line width. Although both samples contain a secondary  $\text{Eu}^{2+}$  phase, integration of the signals at all temperatures shows  $\text{Eu}^{2+}:\text{Eu}^{3+}$  ratios of approximately 70:30, in agreement with the crystal chemical interpretation  $\text{Eu}^{(2+)}_3\text{Eu}^{(3+)}\text{F}_5(\text{CN}_2)_2$ . Over the whole temperature range investigated we observe no significant change of the isomer shift, indicating a stable mixed valency in the temperature range investigated. Similar behavior has been observed for  $\text{Eu}_3\text{F}_4\text{S}_2$ ,<sup>29</sup>  $\text{Eu}_2\text{CuS}_3$ ,<sup>30</sup>  $\text{Eu}_2\text{SiN}_3$ ,<sup>31</sup>  $\text{Eu}_5\text{Sn}_3\text{S}_{12}$ ,<sup>32</sup> or  $\text{Eu}_5\text{Zr}_3\text{S}_{12}$ .<sup>33</sup> Since our Mössbauer spectroscopic setup is restricted in temperature ( $T_{\text{max}} = 330$  K in the bath cryostat) we could not probe for temperature induced valence changes.

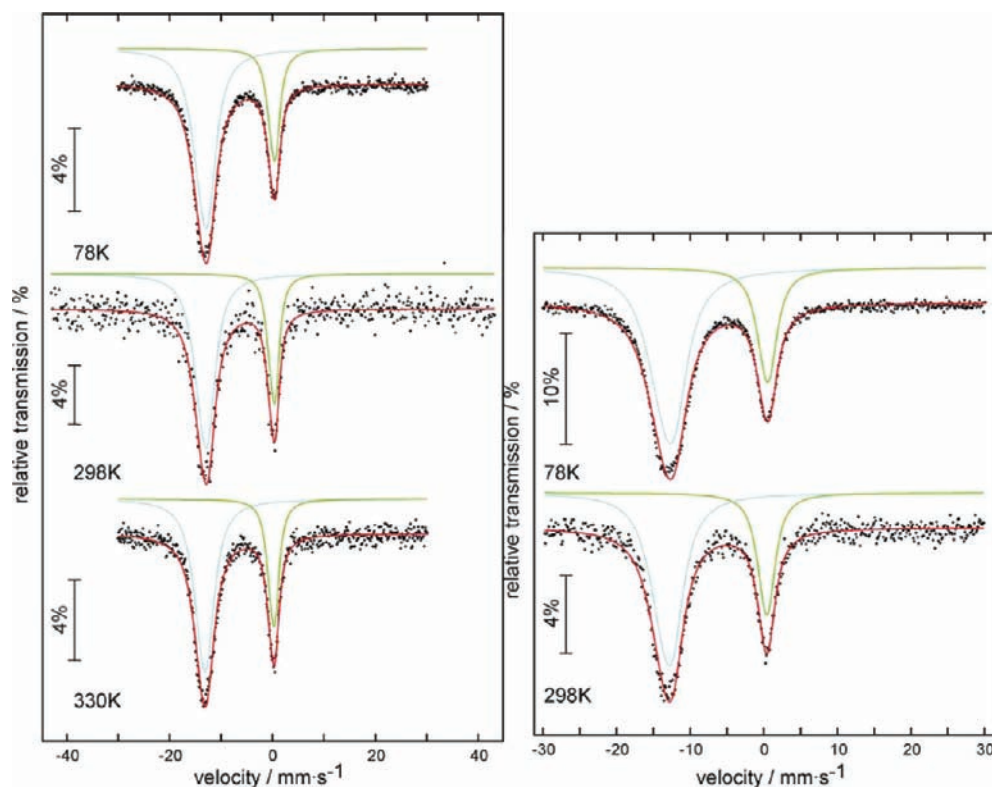


Figure 2. Experimental and simulated  $^{151}\text{Eu}$  Mössbauer spectra of samples I (left) and II (right) of  $\text{Eu}_4\text{F}_5(\text{CN}_2)_2$  at different temperatures.

Table 4. Fitting Parameters of  $^{151}\text{Eu}$  Mössbauer Spectroscopic Measurements of  $\text{Eu}_4\text{F}_5(\text{CN}_2)_2$ <sup>a</sup>

sample	temperature (K)	Eu species	$\delta_1$ ( $\text{mm s}^{-1}$ )	$\Delta E_{\text{Q1}}$ ( $\text{mm s}^{-1}$ )	$\Gamma$ ( $\text{mm s}^{-1}$ )	area (%)
I (+ 20% $\text{EuF}_2$ )	78	$\text{Eu}^{(2+)}$	-13.17(1)	4.8(2)	3.79(6)	74(2)
		$\text{Eu}^{(3+)}$	0.29(2)	2.7(2)	2.12(7)	26(2)
	298	$\text{Eu}^{(2+)}$	-13.12(4)	4.3(6)	3.5(2)	71(2)
		$\text{Eu}^{(3+)}$	0.21(5)	2.9(5)	1.8(2)	29(2)
	330	$\text{Eu}^{(2+)}$	-13.24(2)	3.5(4)	3.72(12)	70(2)
		$\text{Eu}^{(3+)}$	0.19(2)	2.4(3)	2.01(11)	30(2)
II (+10% unknown)	78	$\text{Eu}^{(2+)}$	-13.01(1)	5.4(2)	4.42(6)	73(2)
		$\text{Eu}^{(3+)}$	0.45(1)	2.2(3)	2.75(8)	27(2)
	298	$\text{Eu}^{(2+)}$	-13.10(3)	4.7(3)	3.7(1)	70(2)
		$\text{Eu}^{(3+)}$	0.35(3)	2.0(6)	2.5(2)	30(2)

<sup>a</sup> Numbers in parentheses represent the statistical errors in the last digit. ( $\delta$ ), isomer shift; ( $\Delta E_{\text{Q}}$ ), electric quadrupole splitting; ( $\Gamma$ ), experimental line width.

**Crystal Structure.** Considering the arrangement of the europium ions in the structure of  $\text{Eu}_4\text{F}_5(\text{CN}_2)_2$ , at least three structural patterns may be considered for their description. The *a,b*-projection of the tetragonal structure may be viewed to contain columns of edge-sharing tetrahedral chains formed by the europium atoms, or square antiprismatically arranged europium atoms forming columns parallel to the *c*-axis direction (Figure 3). The combination of these two designs yields the beautiful pattern of two interpenetrating hexagonal sheets of europium atoms, each of them following the motif of a graphite-related structure, in which two orthogonal sets of layers interpenetrate into each other, with a section of this arrangement emphasized in Figure 4. We note here, that the guidelines drawn

between europium atoms do not represent Eu–Eu bonding, as can be assumed by the corresponding interatomic distances of no less than 3.69 Å.

Carbodiimide ions are stacked inside the channels of square antiprismatically arranged columns of europium ions. Surprisingly, the alignment of [NCN] units in the structure is different from what may be regarded when considering an apparently uniform environment with europium ions. The [NCN] ions adopt three europium neighbors at both terminal nitrogen atoms (Figures 5 and 6). However, we note different types of [NCN] units being represented by carbon atoms C1, C2, and C3, each of them being stacked parallel to the *c*-axis direction. Following this direction, the carbodiimide units belonging to C3 show

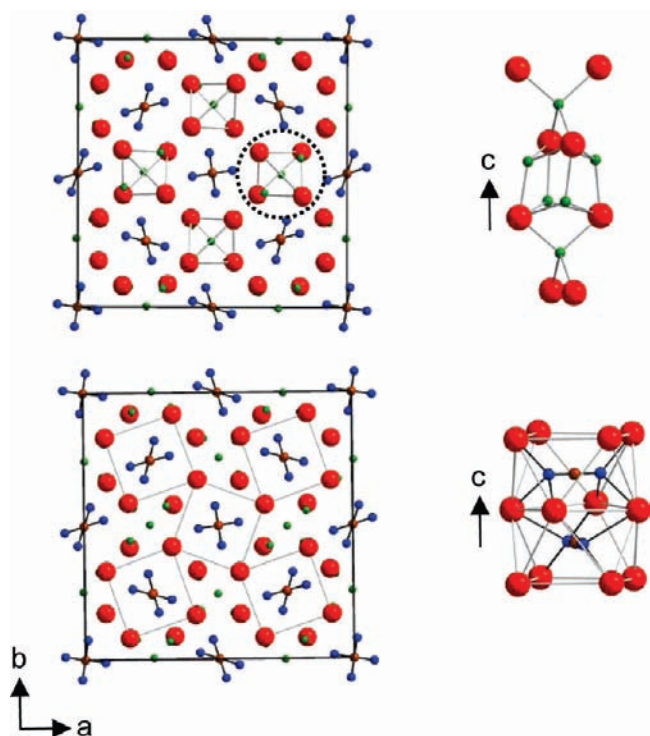


**Figure 3.** Two projections of the  $\text{Eu}_4\text{F}_5(\text{CN}_2)_2$  structure onto the tetragonal plane with the unit cell shown. Columns of fluoride centered europium tetrahedra capped or centered by fluorine atoms (top) and square antiprismatic columns of europium atoms hosting carbodiimide ions (bottom) are emphasized separately. Color code: Eu atoms are shown in red, F atoms green, C atoms brown, and N atoms blue.

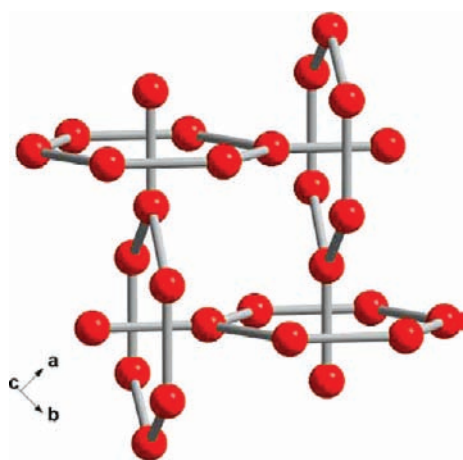


**Figure 4.** Structural arrangement of europium atoms in the structure of  $\text{Eu}_4\text{F}_5(\text{CN}_2)_2$  forms the motif of two interpenetrating sets of graphite-like layers.

alternating rotations (around the  $c$ -axis direction) by  $90^\circ$ . Clearly different rotations are obtained for  $[\text{NCN}]$  units belonging to C2 and C1 (Figures 5 and 6). This unusual orientation behavior of  $[\text{NCN}]$  units becomes more plausible when analyzing their surroundings with europium atoms.

The crystal structure of  $\text{Eu}_4\text{F}_5(\text{CN}_2)_2$  contains four crystallographically distinct europium ions. As we will see below, the  $\text{Eu}-\text{F}$  and  $\text{Eu}-\text{N}$  bond lengths around Eu1 are clearly shorter

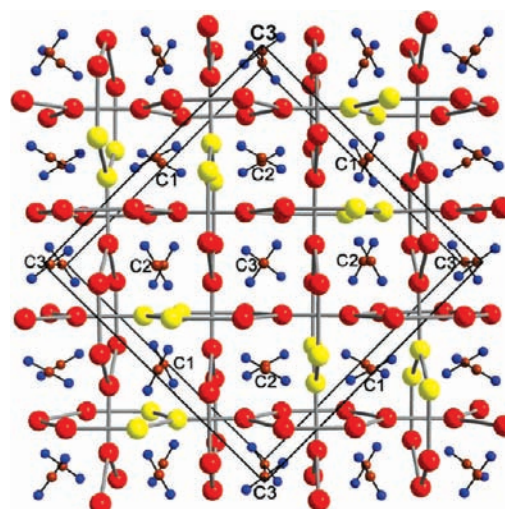


**Figure 5.** Distribution of Eu1 shown in yellow and of Eu2, Eu3, and Eu4 shown in red color in the structure of  $\text{Eu}_4\text{F}_5(\text{CN}_2)_2$  (fluorine atoms are omitted). Color code: Eu1 are shown in yellow, Eu2, Eu3, and Eu4 are shown red, C atoms are brown, and N atoms are blue.

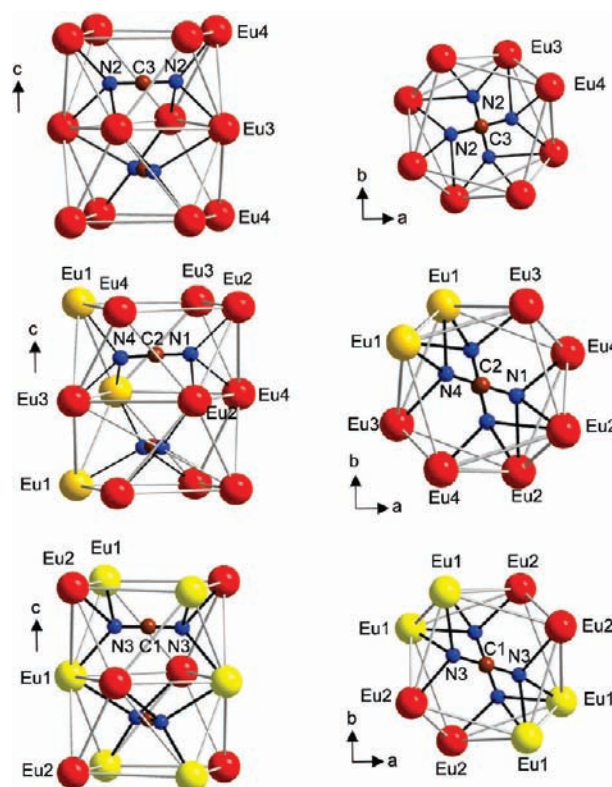


**Figure 6.** Sections of square antiprismatic columns of europium ions in the structure of  $\text{Eu}_4\text{F}_5(\text{CN}_2)_2$  hosting the  $[\text{NCN}]$  units. The  $[\text{NCN}]$  units belonging to C3 have no Eu1 neighbor, those belonging to C2 tend to adjust toward the Eu1 neighbors on one end, and those belonging to C1 tend to adjust to Eu1 neighbors on two ends. Color code: Eu1 is shown in yellow, Eu2, Eu3, and Eu4 are shown red, C atoms are brown, and N atoms are blue.

than those of the other Eu ions, suggesting that Eu1 represents the trivalent ion in mixed-valent  $\text{Eu}^{(2+)}_3\text{Eu}^{(3+)}\text{F}_5(\text{CN}_2)_2$ . When we emphasize the trivalent Eu1 ions as shown (in yellow color) in

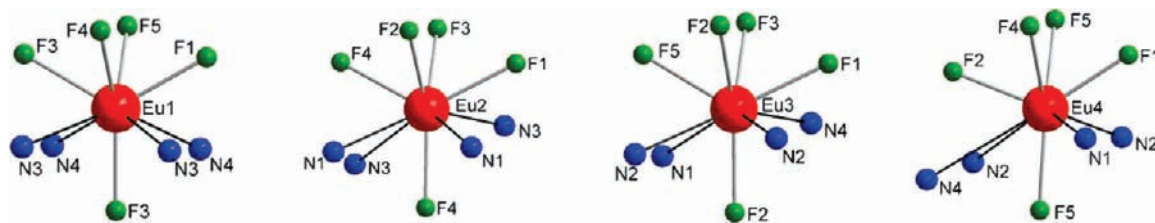


**Figure 7.** Coordination environments around europium ions in  $\text{Eu}_4\text{F}_5(\text{CN}_2)_2$ . Note that some of the Eu–N connecting lines shown appear unreasonably long.

the structure drawing of Figures 5 and 6, the alignment of the [NCN] units becomes conclusive, because we note that their [N–C–N] bonding axes always tend to point toward the direction of trivalent Eu1 ions. However, the carbodiimide ion [N2–C3–N2] has no direct Eu1 neighbor and shows an orthogonal stacking alternation parallel to the *c*-axis repeat with an equal number of Eu3 and Eu4 neighbors at both terminal nitrogen atoms of [NCN], yielding two equivalent C–N distances of 1.212(8) Å. In contrast, the presence of Eu1 from only one end of the [N4–C2–N1] unit yields a small imbalance of C–N bond lengths of 1.233(9) and 1.201(9) Å. This discrepancy is small enough to consider still a carbodiimide (instead of cyanamide) ion here, too. The third carbodiimide unit [N3–C1–N3] is surrounded by Eu(1) from both ends, and thus being fully symmetric with two equivalent C–N distances of 1.225(9) Å (Figure 6).

An analysis of the coordination environments of the four distinct europium atoms in the structure supports the assumption of separate lattice sites for divalent and trivalent europium ions in the structure of mixed-valent  $\text{Eu}^{(2+)}_3\text{Eu}^{(3+)}\text{F}_5(\text{CN}_2)_2$ . Divalent and trivalent europium ions can be usually distinguished in structures by the numbers and distances of surrounding atoms, as implied by lower coordination numbers and shorter bond lengths for  $\text{Eu}^{3+}$  compared with  $\text{Eu}^{2+}$ .

All europium ions in the structure of  $\text{Eu}_4\text{F}_5(\text{CN}_2)_2$  exhibit more or less distorted tricapped trigonal prismatic environments formed by a core of five fluorine atoms and four nitrogen atoms of carbodiimide ligands (Figure 7). This observation is particularly interesting because similar environments of differently charged europium ions in a crystal structure may open up perspectives for charge delocalizations. However, distances around Eu1 are significantly shorter and more uniform when compared with those of Eu2, Eu3, Eu4, as can be seen in Figure 7, with selected distance values given in Table 3. For example, average values of Eu–F distances between Eu1, Eu2, Eu3, and Eu4 and their five fluoride neighbors in each case amount to 2.403 Å, 2.505 Å, 2.531 Å, and 2.511 Å. The environments of Eu2, Eu3, and Eu4 with nitrogen atoms are strongly distorted (Figure 6) with only the nearest Eu–N distances (<3 Å) being considered in Table 3. Average Eu–N distances of Eu1, Eu2, Eu3, and Eu4 with their corresponding nitrogen atoms in each case amount to 2.606 Å, 2.749 Å, 2.751 Å, and 2.605 Å, when counting only the next nearest (4, 3, 3, 2) nitrogen neighbors, or to 2.606 Å, 2.950 Å, 2.858 Å, and 3.092 Å, when counting all four nitrogen neighbors in each case as displayed in Figure 7. The pronounced difference in next neighbor distances of Eu1 on one hand and of Eu2, Eu3, and Eu4 on the other hand is in line with the observed values in other mixed-valent europium compounds, such as  $\text{Eu}_2\text{O}_2\text{Br}$ .<sup>22</sup>

Summing up, a distinction between divalent and trivalent europium ions in  $\text{Eu}_4\text{F}_5(\text{CN}_2)_2$  is indicated by the orientation

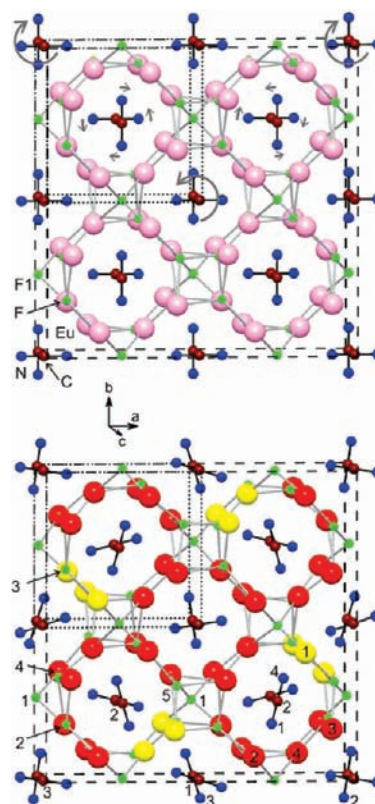


**Figure 8.** Idealized structure (top) of  $\text{Eu}_4\text{F}_5(\text{CN}_2)_2$  with the  $a/2$ ,  $b/2$  subcell emphasized by the dotted square as compared with the refined structure (bottom). In the hypothetical high temperature phase (top)  $\text{Eu}^{2+}$  and  $\text{Eu}^{3+}$  would not be distinguishable (shown in pink), in contrast to the ordered room temperature phase (bottom) where  $\text{Eu}^{3+}$  (yellow) and  $\text{Eu}^{2+}$  (red) occupy different sites. Positions of Eu and C compare with those of Al and Cu, respectively, of  $\text{CuAl}_2$ , whereas the theoretical N and F positions (50% occupancy) are vacant in  $\text{CuAl}_2$ . Note, for the sake of clarity, not all F and N positions are drawn in the upper drawing. Europium and fluorine atoms are connected to guide the eye. The tilting and rotation mode of the [NCN] groups is indicated by arrows. Numbering in the lower part drawing of the fully ordered structure corresponds to the atom designations (Table 2).

behavior of the [N–C–N] ions in the structure. A charge assignment in the structure can be based on significantly shorter distances around Eu1. Finally, the crystal structure of  $\text{Eu}_4\text{F}_5(\text{CN}_2)_2$  exhibits similar coordination environments around divalent and trivalent europium ions in the structure, as displayed in Figure 6. The presence of similar Eu ions and rotated [N–C–N] anions in the structure challenges a perspective examination on a hypothetical high-symmetry scenario of the  $\text{Eu}_4\text{F}_5(\text{CN}_2)_2$



structure. A phase-transition into a high-symmetry structure considered by us would be regarded to involve a displacive transformation particularly of carbodiimide anions following a second order phase-transition. Differential thermal analysis (DTA) studies of  $\text{Eu}_4\text{F}_5(\text{CN}_2)_2$  have shown a very weak endothermic effect with an onset temperature near 360 °C on heating and an exothermic effect near 340 °C on cooling which cannot safely be addressed to  $\text{Eu}_4\text{F}_5(\text{CN}_2)_2$  because it could be also due to an impurity phase. The X-ray diffraction patterns calculated for both the crystal structure and the hypothetical high-symmetry structure (see below) are practically identical, making a high-temperature X-ray powder diffraction study needless, whereas a neutron diffraction study could certainly help.

**Hypothetical High-Symmetry Structure of  $\text{Eu}_4\text{F}_5(\text{CN}_2)_2$ .** The arrangement of the europium ions within the refined crystal structure of  $\text{Eu}_4\text{F}_5(\text{CN}_2)_2$  follows a symmetry higher than the space group symmetry (see Figure 4) and does not allow a firsthand differentiation between individual charges of europium ions in the structure. In addition, the four crystallographically distinct positions of the europium atoms, displayed in Table 2, suggest a potentially more evenly arranged europium substructure when trying to relate some europium positions by symmetry (see related positions of Eu1 and Eu3 or Eu2 and Eu4, respectively).

A reduced tetragonal unit cell was modeled for  $\text{Eu}_4\text{F}_5(\text{CN}_2)_2$  with  $a' = a/2$  and  $b' = b/2$  with just one crystallographic europium atom position. This position turned out to be similar to the position of the aluminum atom in the intermetallic compound  $\text{CuAl}_2$  (space group  $I4/mcm$ ). On the basis of this model, all carbon atoms of the carbodiimide ions would occupy positions similar to the Cu atoms in the  $\text{CuAl}_2$  type structure, displayed in Figure 8.

The structural relationship between a hypothetical high-symmetry structure<sup>34</sup> and the refined structure was examined in more detail by a group-subgroup scheme (Figure 9) following the *Bärnighausen* formalism.<sup>35</sup> Departing from the  $\text{CuAl}_2$  type structure, space group  $I4/mcm$ , all fluorine sites and all nitrogen sites of the  $\text{Eu}_4\text{F}_5(\text{CN}_2)_2$  model would be statistically occupied by 50%, and the symmetry reduction proceeds via two *klassengleich*, one isomorphic, and one *translationengleich* symmetry reduction to the noncentrosymmetric space group  $P4_21c$ . The last step causes the possibility of twinning by inversion. A splitting of the europium site, enabling an ordering of di- and trivalent europium ions may occur after the second symmetry reduction, but the required 3:1 ratio of di- and trivalent europium ions is possible for the first time in the space group  $P4/mnc$  (Figure 9). The last step of the symmetry reduction ( $P4/mnc \rightarrow P4_21c$ ) leads to a complete ordering (occupied vs unoccupied sites) of the nitrogen and fluorine atoms. The fluorine atoms occupy only those positions being not too close to nitrogen atoms. The presence of di- and trivalent europium require the [NCN] groups to be tilted off their ideal orientations (upper part of Figure 8) to comply with the different environments of  $\text{Eu}^{2+}$  and  $\text{Eu}^{3+}$ . The required distortions from the high-symmetry structure to the refined crystal structure are modeled by symmetry reductions where the atoms and [NCN] groups are uncoupled in four steps. This uncoupling resolves more easily by viewing the stacking of [NCN] groups along the *c*-axis direction (lower part of Figure 8). A co-operative rotation of two [NCN] groups around the *c*-axis is done at 0, 0, *z* and at  $1/2, 1/2, z$ , left and right rotation, respectively (Figure 8, top). An opposite rotation of two [NCN] groups is found at  $\pm 1/4, \pm 1/4, z$ . The latter allows a more symmetric arrangement of the [NCN] groups around Eu1.

The comparatively small fluoride ions in this model occupy sites that are closely related to positions reported for deuterium atoms in the structure of  $\text{Th}_2\text{AlD}_{4-x}$ , whose heavy atom structure can be considered isotopic with that of the  $\text{CuAl}_2$ -type structure.  $\text{Th}_2\text{AlD}_{4-x}$  was reported to crystallize with the space groups  $I4/mcm$  or  $P4_2m$ , respectively, depending on the number and distribution of D atoms present in the structure.<sup>36</sup> Thus, the ordering of hydrogen most likely results in another branch of the symmetry tree.

The existence of a substructure for  $\text{Eu}_4\text{F}_5(\text{CN}_2)_2$  having a higher symmetry than the observed in the crystal structure of  $\text{Eu}_4\text{F}_5(\text{CN}_2)_2$  would give rise to an intervalence charge transfer associated with a delocalized mixed-valence structure under certain conditions. A pressure induced phase-transition including a small realignment of [N–C–N] units, associated with a significant volume reduction, was recently shown for  $\text{Tm}_2(\text{CN}_2)_3$ .<sup>14</sup>

## ■ ASSOCIATED CONTENT

**S Supporting Information.** X-ray crystallographic data for  $\text{Eu}_4\text{F}_5(\text{CN}_2)_2$  in CIF format. This material is available free of charge via the Internet at <http://pubs.acs.org>.

## ■ AUTHOR INFORMATION

### Corresponding Author

\*E-mail: [juergen.meyer@uni-tuebingen.de](mailto:juergen.meyer@uni-tuebingen.de).

## ■ ACKNOWLEDGMENT

Support of this Research by the Deutsche Forschungsgemeinschaft (Bonn) through the project *Nitridocarbonate* is gratefully acknowledged.

## ■ REFERENCES

- (1) (a) Meyer, H.-J. *Dalton Trans.* **2010**, 39, 5973–5982. (b) Gibson, K.; Ströbele, M.; Blaschkowski, B.; Glaser, J.; Weisser, M.; Srinivasan, R.; Kolb, H.-J.; Meyer, H.-J. *Z. Anorg. Allg. Chem.* **2003**, 629, 1863–1870.
- (2) Weisser, M.; Tragl, S.; Meyer, H.-J. *Z. Anorg. Allg. Chem.* **2007**, 633, 802–806.
- (3) (a) Weisser, M.; Burgert, R.; Schnöckel, H.; Meyer, H.-J. *Z. Anorg. Allg. Chem.* **2008**, 634, 633–640. (b) Burgert, R.; Weiss, K.; Schnöckel, H.; Weisser, M.; Meyer, H.-J.; v. Schnering, H. G. *Angew. Chem., Int. Ed.* **2005**, 44, 265–269.
- (4) Liu, X.; Krott, M.; Müller, P.; Hu, C.; Lueken, H.; Dronskowski, R. *Inorg. Chem.* **2005**, 44, 3001–3003.
- (5) Liu, X.; Stork, L.; Speldrich, M.; Lueken, H.; Dronskowski, R. *Chem.—Eur. J.* **2009**, 15, 1558–1561.
- (6) Krott, M.; Liu, X.; Fokwa, B. P. T.; Speldrich, M.; Lueken, H.; Dronskowski, R. *Inorg. Chem.* **2007**, 46, 2204–2207.
- (7) Liu, X.; Wanke, M. A.; Lueken, H.; Dronskowski, R. *Z. Naturforsch.* **2005**, B60, 593–596.
- (8) Neukirch, M.; Tragl, S.; Meyer, H.-J. *Inorg. Chem.* **2006**, 45, 8188–8193.
- (9) Unverferth, L.; Glaser, J.; Ströbele, M.; Meyer, H.-J. *Z. Anorg. Allg. Chem.* **2009**, 635, 1947–1952.
- (10) Srinivasan, R.; Glaser, J.; Tragl, S.; Meyer, H.-J. *Z. Anorg. Allg. Chem.* **2005**, 631, 479–483.
- (11) Srinivasan, R.; Ströbele, M.; Meyer, H.-J. *Inorg. Chem.* **2003**, 42, 3406–3411.
- (12) (a) Sindlinger, J.; Glaser, J.; Bettentrup, H.; Jüstel, T.; Meyer, H.-J. *Z. Anorg. Allg. Chem.* **2007**, 633, 1686–1690. (b) Takahashi, M.; Hashimoto, Y.; Kikkawa, S.; Kobayashi, H. *Zairyo* **2000**, 49, 1230–1234. (c) Hölsä, J.; Lamminmäki, R.-J.; Lastusaari, M.; Säilynoja, E.; Porcher,



P. *Spectrochim. Acta A* **1998**, *54*, 2065–2069. (d) Säilynoja, E.; Lastusaari, M.; Hölsä, J.; Porcher, P. J. *Luminescence* **1997**, *72*, 210–203. (e) Hashimoto, Y.; Takahashi, M.; Kikkawa, S.; Kanamaru, F. J. *Solid State Chem.* **1996**, *125*, 37–42. (f) Hashimoto, Y.; Takahashi, M.; Kikkawa, S.; Kanamaru, F. J. *Solid State Chem.* **1995**, *114*, 592–594. (g) Caro, P. J. *Less-Common Met.* **1968**, *16*, 367–377.

(13) Srinivasan, R.; Tragl, S.; Meyer, H.-J. *Z. Anorg. Allg. Chem.* **2005**, *631*, 719–722.

(14) Glaser, J.; Unverfehrt, L.; Bettentrup, H.; Heymann, G.; Huppertz, H.; Jüstel, T.; Meyer, H.-J. *Inorg. Chem.* **2008**, *47*, 10455–10460.

(15) Liao, W.; Hu, C.; Kremer, R. K.; Dronskowski, R. *Inorg. Chem.* **2004**, *43*, 5884–5890.

(16) Liao, W.; Dronskowski, R. *Z. Anorg. Allg. Chem.* **2005**, *631*, 1953–1956.

(17) Liao, W.; Dronskowski, R. *Z. Anorg. Allg. Chem.* **2005**, *631*, 496–498.

(18) The sequence of anions given within a chemical formula should follow alphabetical order (IUPAC). The problem using this rule becomes evident when considering a metal carbodiimide chloride and a metal bromide carbodiimide, or even more when a carbodiimide ion is distorted to represent a cyanamide, and should be therefore denoted as metal chloride cyanamide. Within the framework of this research we refer to the notation “metal halide carbodiimide” or “metal halide carbodiimide nitride” when an additional nitride is present.

(19) Reckeweg, O.; DiSalvo, F. J. *Z. Anorg. Allg. Chem.* **2003**, *629*, 177–179.

(20) Unverfehrt, L.; Glaser, J.; Ströbele, M.; Tragl, S.; Gibson, K.; Meyer, H.-J. *Z. Anorg. Allg. Chem.* **2009**, *635*, 479–483.

(21) Röhler, J.; Kaindl, G. *Solid State Commun.* **1980**, *36*, 1055–1057.

(22) Hammerich, S.; Pantenburg, I.; Meyer, G. *Z. Anorg. Allg. Chem.* **2006**, *632*, 1487–1490.

(23) Wickleder, C. *Z. Naturforsch.* **2002**, *57b*, 901–907.

(24) Wickleder, C.; Hartenbach, I.; Lauxmann, P.; Schleid, T. *Z. Anorg. Allg. Chem.* **2002**, *628*, 1602–1606.

(25) Tanguy, B.; Portier, J.; Vlasse, M.; Pouchard, M. *Bull. Soc. Chim.* **1972**, *3*, 946–950.

(26) Sheldrick, G. M. *Acta Crystallogr., Sect. A: Found. Crystallogr.* **2008**, *64*, 112–122.

(27) Lueken, H. *Magnetochemie*; Teubner: Stuttgart, Germany, 1999; pp 38, 153, 273.

(28) Ehnholm, G. J.; Katila, T. E.; Lounasmaa, O. V.; Reivari, P.; Kalvius, G. M.; Shenoy, G. K. *Z. Phys.* **1970**, *235*, 289–307.

(29) Grossholz, H.; Hartenbach, I.; Kotzyba, G.; Pöttgen, R.; Trill, H.; Mosel, B. D.; Schleid, T. *J. Solid State Chem.* **2009**, *182*, 3071–3075.

(30) Furuuchi, F.; Wakeshima, M.; Hinatsu, Y. *J. Solid State Chem.* **2004**, *177*, 3853–3858.

(31) Zeuner, M.; Pagano, S.; Matthes, P.; Bichler, D.; Johrendt, D.; Harmening, T.; Pöttgen, R.; Schnick, W. *J. Am. Chem. Soc.* **2009**, *131*, 11242–11248.

(32) Jakubcová, P.; Johrendt, D.; Sebastian, C. P.; Rayaprol, S.; Pöttgen, R. *Z. Naturforsch.* **2007**, *62b*, 5–14.

(33) Jakubcová, P.; Schappacher, F. M.; Pöttgen, R.; Johrendt, D. *Z. Anorg. Allg. Chem.* **2009**, *635*, 759–763.

(34) Note that the high-symmetry structure of  $\text{Eu}_4\text{F}_5(\text{CN})_2$  may not be consistent with the space group of  $\text{CuAl}_2$  ( $I4/mcm$ ). A symmetry optimization of the  $a' = a/2$ ,  $b' = b/2$ ,  $c' = c$  subcell of  $\text{Eu}_4\text{F}_5(\text{CN})_2$  without F disorder yielded the space group  $I\bar{4}2m$  ( $Z = 2$ ), with a 100% match by MISSYM; Le Page, Y. J. *Appl. Crystallogr.* **1987**, *20*, 264–269. **1988**, *21*, 983–984.

(35) (a) Bärnighausen, H. *Commun. Math. Chem.* **1980**, *9*, 139. (b) Bärnighausen, H.; Müller, U. *Symmetriebeziehungen zwischen den Raumgruppen als Hilfsmittel zur straffen Darstellung von Strukturzusammenhängen in der Kristallchemie*; University of Karlsruhe and University/GH Kassel: Karlsruhe, Germany, 1996; (c) Müller, U. *Z. Anorg. Allg. Chem.* **2004**, *630*, 1519–1537.

(36) Sorby, M. H.; Fjellvag, H.; Hauback, B. C.; Maeland, A. J.; Yartys, V. A. *J. Alloys Compd.* **2000**, *309*, 154–164.